Microevaporators with accumulators for the screening of phase diagrams of aqueous solutions

P. Moreau, J. Dehmoune, J.-B. Salmon, and J. Leng[a)]
Laboratory of the Future (CNRS/Rhodia UMR 5258), Université Bordeaux-1, 33608 Pessac, France

(Received 23 April 2009; accepted 31 May 2009; published online 21 July 2009)

We design near-autonomous microfluidic devices for concentrating aqueous solutions steadily over days in a very controlled manner. We combine suction pumps that drive the solution and concentrate it steadily, with a nanoliter-sized storage pool where the solute accumulates. The fine balance between advection and diffusion in the pump and diffusion alone in the accumulation pool yields several filling regimes. One of them is universal as being steady and independent of the solute itself. It results a specific equivalence between time and concentration, which we use to build the phase quantitative diagram of a ternary aqueous solution on nanoliter scale. © *2009 American Institute of Physics*. [DOI: 10.1063/1.3159811]

Building the phase diagram of a multicomponent system is a prerequisite in many fields ranging from soft matter, crystallization for proteomics, industrial formulation, etc., along with a need for the general understanding. It is a somewhat tedious and repetitive task where the added value mostly lies in the final object, not the preparation, and for this reason automated formulators such as robotic plateforms are very convenient.[1] Recently, miniaturized tools such as microfluidic lab-on-a-chip devices have started to help screening the phase behavior of complex systems, especially for biological samples.[2] The most recent microfluidic plateforms nearly all use integrated evaporation as a convenient way to increase the concentration in a nanoliter-sized test tube. Evaporation is indeed a powerful paradigm for guiding self-assembly[3] and in the present work, we exploit a gentle and miniaturized bottom up self-assembly principle[4–6] to design near-autonomous microfluidic devices that drains and concentrates aqueous solutions steadily over days in a very controlled manner. We demonstrate they can be used for the quantitative screening of the phase behavior of multicomponent systems with minute consumption and economy of analysis.

The very basis of this work relies on suction pumps, which can for instance drain water from a reservoir by evaporation across the wall of veins.[7] Permeation of water lowers the pressure of water, which induces a flow.[8] The ultimate engine driving the process remains evaporation, which is slaved to the outer atmosphere outside the device, which we assume unsaturated and actually dry. In recent elastomeric microfluidic geometries [mostly made out of Poly(DimethylSiloxane), PDMS], the evaporation not only causes the solution to flow[6,9] at small velocity ($\sim \mu$m s^{-1}) but also concentrates it.[10] The pumps work as a solute source delivering an exact and steady current of solutes, anywhere below μM/h.[4] We call t_e the time needed to evaporate V_c, the volume of one pumping channel (see Fig. 1, with $V_c = L_0 wh$). After t_e, the channel has been replenished with fresh solution from the reservoir; the rate of solute molecules N_s entering the pump is $\dot{N}_s = c_0 V_c / t_e$ where c_0 is the concentration of the solution in the reservoir. More specifically, the solute is actually trapped around the tip of the pump at a distance $p \sim (Dt_e)^{1/2}$ that results from an advection-diffusion competition[4] with D the diffusion coefficient of the solute. The competition also predicts that the concentration gradient follows a Gaussian profile. Being continuously fed from the reservoir, the concentration around the tip raises like $c(x,t) \sim t \times \exp(-x^2/2p^2)$, where x is the distance from the tip, to a very good degree of precision asymptotically for ideal solutions[4] while a general theory is provided in Ref. 11 for any type of mixture. The actual concentration rate results from the conservation of the solute, which does not evaporate. We define V_{ad} the advection-diffusion volume in which the solute is stored (in the case of a Gaussian gradient, $V_{ad} = \sqrt{\pi/2} pwh$). After a transient regime lasting τ_e $[\sim t_e \ln(L_0/p)]$,[5] the pump starts delivering a steady current in V_{ad}. The concentration trajectory at the tip of the device thus follows $c \sim c_0 (V_c/V_{ad})(t/t_e)$, a simple law that makes it robust but still dependent on the solute properties via V_{ad}.

We now connect the linear evaporator to a storage pool, which is not under the evaporation membrane (Fig. 1). As

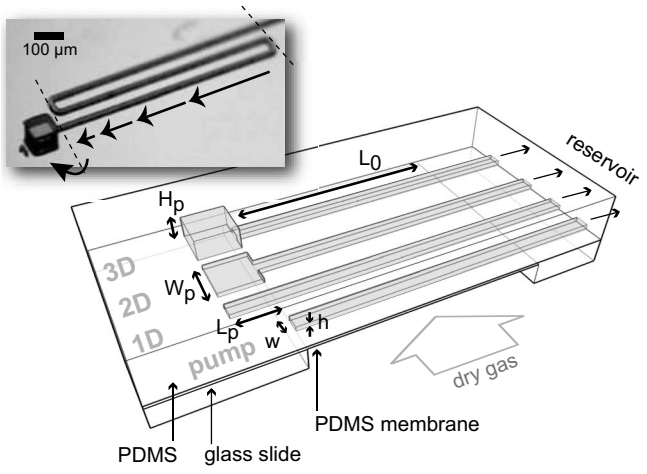

FIG. 1. Sketch of the storage device which connects a solute pump (a linear evaporator in contact with a membrane) to a storage pool sheltered from evaporation. The inset shows a master mold made of photoresist on silicon, which is then replicated into PDMS and sealed with a PDMS membrane. The straight arrows on the picture represent the magnitude of the velocity field induced by evaporation.

a)Electronic mail: jacques.leng-exterieur@eu.rhodia.com.

there is no evaporation in this zone, diffusion is only able to equilibrate concentration gradients. The latter are generated at the entrance of the pool by the pump and relax in a typical time scale $\tau_d \sim l_p^2/D$ where l_p is a typical (the longest) length of the pool. Whether these gradients are allowed to equilibrate or not is selected by the kinetic properties of pump, namely, its rapidity to drive solute at its tip. We confirmed with numerics (not shown) the intuitive result that there is crossover between two filling regimes. If diffusion is slow compared to feed ($\tau_e \ll \tau_d$), the solute accumulates at the entrance of the pool and the gradients develop and amplify on the time scale of τ_e. When diffusion is efficient at equilibrating the excess of solute that enters in the pool ($\tau_d \ll \tau_e$), gradients remain as a consequence of flow but they become relatively fainter with time ($\delta c/c \sim 1/t$). In this evaporative filling regime, the pool is nearly homogeneously filled, and its concentration rate is slaved to the pump, which delivers a steady current of solute, which we assume for the rest of the work.

The second consequence of adding an extra volume V_p at the tip of the evaporator is a dilution effect; in a stationary mode ($\dot{c}=0$), where no solution enters the device but pure water confines the solute at the tip of the device, an exact solution of the concentration profile is simply given by a flat profile in the pool and a Gaussian profile in the feeding arm. The solute that was trapped in V_{ad} before the adjunction of a pool has now access to V_p+V_{ad}. We thus expect the concentration at the tip of the device to be corrected by a partitioning factor,

$$\mathcal{R} = \frac{V_p}{V_p + V_{\mathrm{ad}}}, \tag{1}$$

as compared to the storage in the bare pump. $\mathcal{R}$ expresses the amount of solute stored in the pool as compared to the total sent in the device, and we found numerically and experimentally that even if there are gradients that remain during the evaporative filling regime, we may define unambiguously a dynamic partitioning factor $\mathcal{R}$ during the filling procedure, and that it converges asymptotically ($t \gg \tau_e$) toward the static definition of Eq. (1). We thus measured the latter in two-dimensional (2D) pools of many different shapes and with fluorescent species of calibrated mobilities (Fig. 2). We observe an excellent agreement between the measurements and prediction and we therefore use the partitioning factor as a guide to estimate the concentration in the pool against time,

$$c \approx c_0 \mathcal{R} \frac{V_c}{V_p} \frac{t}{t_e} \tag{2}$$

at $t \gg \tau_e \gg \tau_d$. The solute is continuously transferred from the channel to the tip and then into the pool at a rate $V_c/V_p t_e$ modulated by the partitioning ratio $\mathcal{R}$. Interestingly, if $\mathcal{R} \to 1$, $\dot{c}/c_0$ becomes solute independent, and the device can then store any type of solute at the same rate. The concentration in the pool also becomes less sensitive to the possible variations of both evaporation conditions and solute properties (e.g., nonideality). It yields a universal filling regime, which depends only on a device parameter t_e that we may calibrate independently. This limit is reached in the case of three-dimensional (3D) pools.

We use the device to study a real phase diagram: Poly-(EthyleneGlycol) of weight 3.35 kDa and ammonium sulfate in water at room temperature. We first design a device with

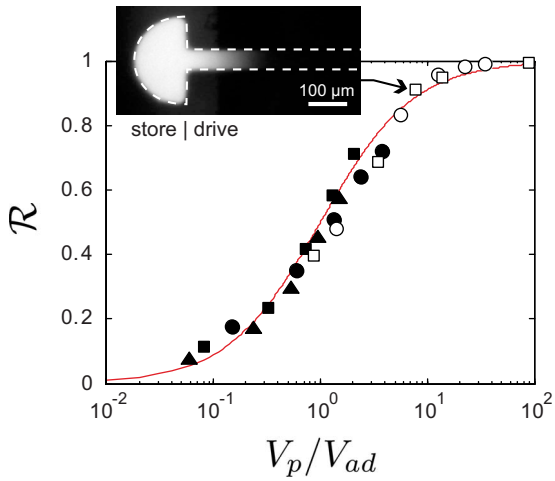

FIG. 2. (Color online) Static filling ratio $\mathcal{R}$ measured by image analysis for several solutes (solid symbols for fluorescein, open symbols for 100 nm diameter fluorescein-labeled colloids) in various geometries (semicircular pools of radius 50, 100, 150, 200, and 250 μm and feeding arms of width $w=30$, 50, and 100 μm) and expressed as a function of a dimensionless parameter V_p/V_{ad} where V_{ad} is calculated after independent calibration. The solid line represents Eq. (1).

$\tau_d \ll \tau_e$ and with $\mathcal{R} \approx 1$ ($\mathcal{R} \approx 0.95$ and ≈ 0.98 with $D \approx 8.8$ and $1.7 10^{-10}$ m^2 s^{-1} for polymer and salt, respectively; typical dimensions are $L_0=5$ mm, $w=50$ μm, and $h \approx 15$ μm for the pump and $H_p=150$ μm and $L_P=W_p=200$ μm). We calibrate the device[5] and find $t_e=460 \pm 20$ s. The chemicals we used are ammonium sulfate and PEG 3.35 kDa used as purchased and dissolved in de-ionized water. In order to reach quasistatic and asymptotic filling conditions, we also require that any transition that may occur during the concentration process happens at $t \gg \tau_e$. It translates into a concentration constraint that permits to define an adequate initial concentration c_0; we use an initial concentration of $\approx 0.2\%$, which shall ensure the asymptotic requirement above 1%. This initial mass fraction is kept constant and we varied the ratio polymer/salt to access a set of different trajectories upon concentration. Figure 3 displays the typical observation of the phase sequence: starting from a homogeneous system, it takes a certain time [t^*, Figs. 3(b) and 3(c)] before a liquid-liquid transition takes place. After this transition, the system remains under evaporation and is still enriched with the solutes; the size of the two domains evolves [Figs. 3(d)–3(f)], and crystallization of the salt phase occurs [Fig. 3(g)].

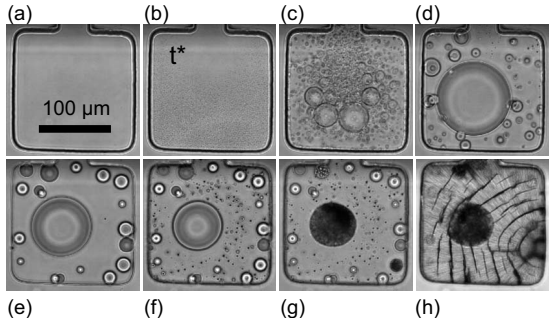

FIG. 3. Series of micrographs showing a sequence of events taking place in a 2D solute pool initially filled with a dilute aqueous solution of PEG 3.35 kDa and ammonium sulfate (at 1% w/w each). As time passes, several transitions are visible and we note t^* the time at which the liquid-liquid transition occurs (b) (enhanced online). [URL: http://dx.doi.org/10.1063/1.3159811.1]

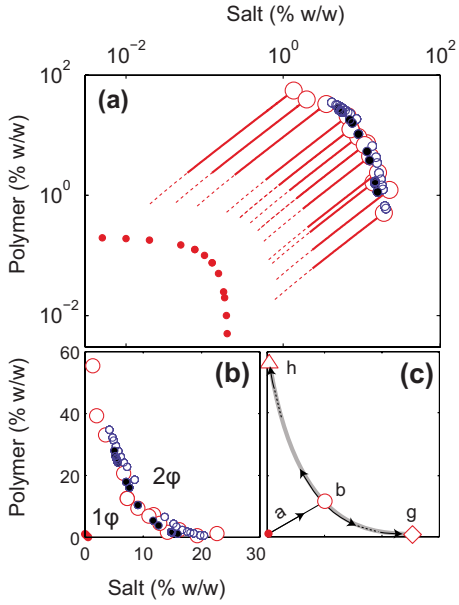

FIG. 4. (Color online) (a) Phase diagram of PEG 3.35 kDa/$(NH_4)_2SO_4$/water built from the kinetic analysis: the initial solutions are prepared at low concentration (red dots) and are concentrated in the microfluidic device; each transition concentration (red large circles) is calculated from the theoretical trajectory, Eq. (2). The latter is plotted for $t > 3\tau_e$ (dotted line) and $t > 10\tau_e$ (solid line) for all initial conditions. The blue and black small circles are thermodynamic equilibrium measurements extracted from Ref. 12 for PEG 2 kDa and PEG 4 kDa, respectively. Graph (b) shows the same results in a linear scale and graph (c) is a schematic analysis of the full pathway where letters refer to Fig. 3.

Ultimately, we recognize the solidification of the polymer-rich zone to the typical texture of the semicrystalline polymer [Fig. 3(h)]. Quantitatively and based on the time-concentration equivalence, we obtain the kinetic diagram of Fig. 4 where the initial conditions are displayed as red dots at low concentrations and where calculated trajectories end up at t^* at the liquid/liquid transition, which we translate into a concentration (open circles). Remarkably, the nearby blue dots are data extracted from equilibrium measurements[12] and agree very well with our kinetic results. It is therefore possible to use a simplified picture [Eq. (2)] even though the system is complex and not ideal.

While we illustrated here the procedure for building a real and quantitative phase diagram of a water soluble polymer in brine out of a dilute solution, our tools may also serve another goal: bottom-up self-assembly. Indeed, the transpiration-based pumps rely on environment only (with a relative humidity < 1) to transfer momentum to the fluid;[8] it inspired recent microfluidic strategies biomimicking vascular plants that demonstrate the ability to deliver ultrasmall currents ($\sim$nl/h) and to sustain large pressure drops steadily over days.[8,13] We now add up a concomitant and spontaneous feature, which can be optimized: the possibility to extract the solutes of a dilute solution and to deliver them nonspecifically toward dedicated zones where they can be processed further, as for instance with a chemical reaction.

We gratefully acknowledge Armand Ajdari for his original idea of the accumulation pool and thank Rhodia, Région Aquitaine, and Agence Nationale de la Recherche (grant DNA-TOOL of the ANR-07-NANO-001-02 program) for funding and support.

[1] A. Imberg and S. Engstrom, Colloids Surf., A **221**, 109 (2003).
[2] J. Leng and J.-B. Salmon, Lab Chip **9**, 24 (2009).
[3] G. Ozin, A. Arsenault, and L. Cademartiri, *Nanochemistry: A Chemical Approach to Nanomaterials* (RSC, Cambridge, 2009).
[4] J. Leng, B. Lonetti, P. Tabeling, M. Joanicot, and A. Ajdari, Phys. Rev. Lett. **96**, 084503 (2006).
[5] J. Leng, M. Joanicot, and A. Ajdari, Langmuir **23**, 2315 (2007).
[6] G. Randall and P. Doyle, Proc. Natl. Acad. Sci. U.S.A. **102**, 10813 (2005).
[7] V. Namasivayam, R. Larson, D. Burke, and M. Burns, J. Micromech. Microeng. **13**, 261 (2003).
[8] T. Wheeler and A. Stroock, Nature (London) **455**, 208 (2008).
[9] E. Verneuil, A. Buguin, and P. Silberzan, Europhys. Lett. **68**, 412 (2004).
[10] J. Shim, G. Cristobal, D. Link, T. Thorsen, Y. Jia, K. Piattelli, and S. Fraden, J. Am. Chem. Soc. **129**, 8825 (2007).
[11] M. Schindler and A. Ajdari, Eur. Phys. J. E **28**, 27 (2009).
[12] Y. Gao, Q. Peng, Z. Li, and Y. Li, Fluid Phase Equilib. **63**, 157 (1991).
[13] X. Noblin, L. Mahadevan, I. Coomaraswamy, D. Weitz, N. Holbrook, and M. Zwieniecki, Proc. Natl. Acad. Sci. U.S.A. **105**, 9140 (2008).